Supplementary Information

Structure and Molecular Mechanism of Signaling for the Glucagon-like Peptide-1 Receptor Bound to Gs Protein and Exendin-P5 Biased Agonist

Bo Li,† Krystyna Maruszko,† Soo-Kyung Kim,† Moon Young Yang, Amy-Doan P Vo, William A. Goddard III*

Division of Chemistry and Chemical Engineering and Materials Process and Simulation Center, California Institute of Technology, Pasadena, CA 91125.

†These authors contributed equally.

*Corresponding author, e-mail: wag@caltech.edu

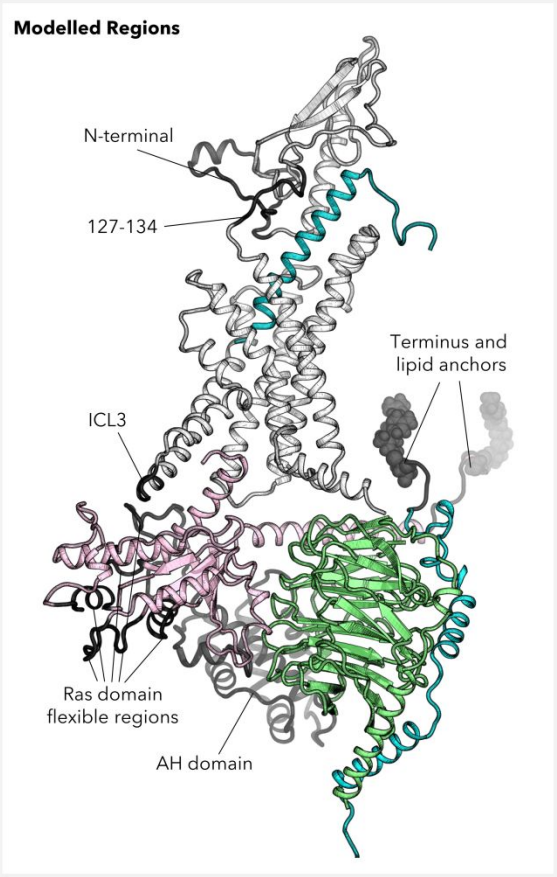

Figure S1. Depiction of remodeled structures from our present simulations (colored in black). A detailed outline of the computationally added structures is provided in the Method Section.

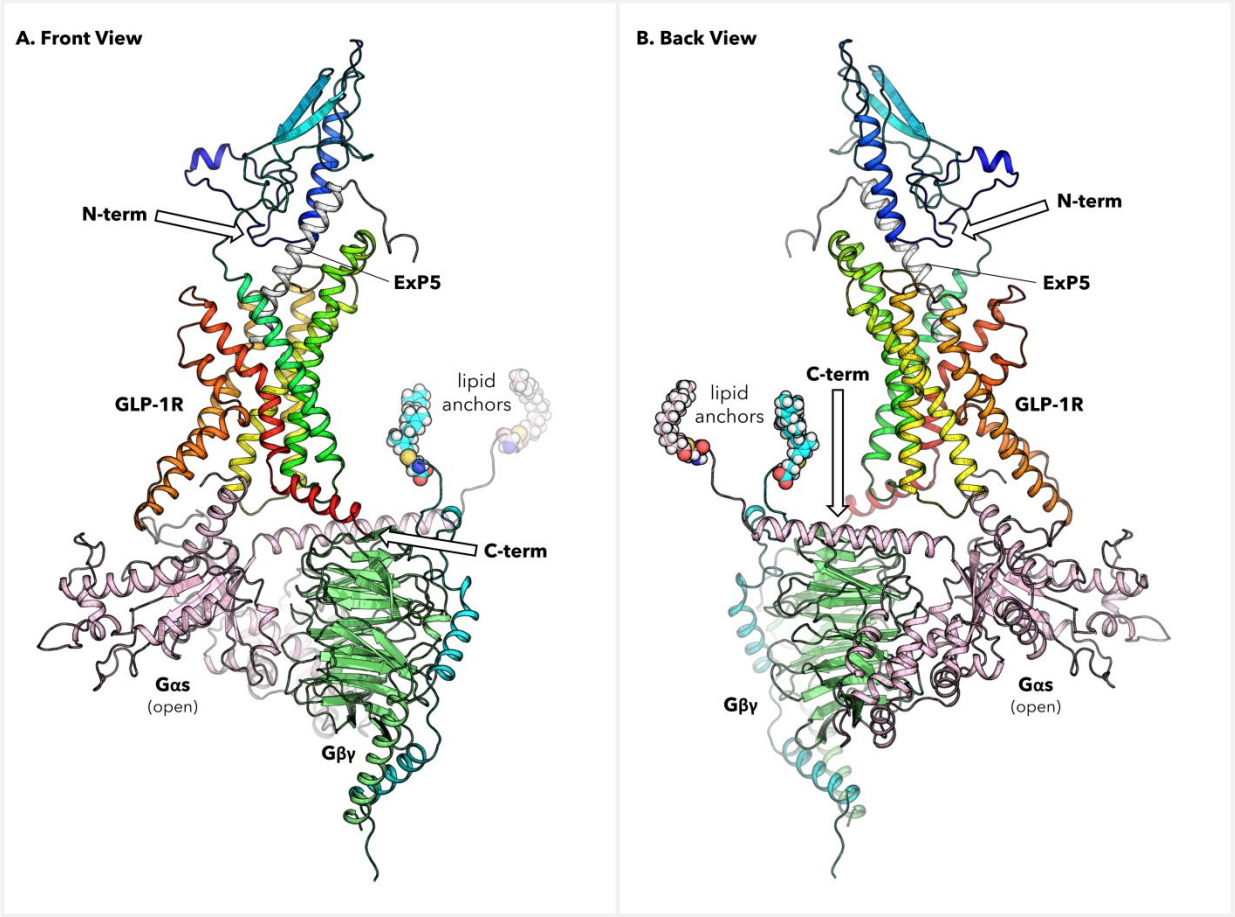

Figure S2. Structure overview of the ExP5 biased agonist-bound GLP-1R–Gs signaling complex. (A-B) Front and back views with GLP-1R colored by residue number (blue: N-terminus, red: C-terminus).

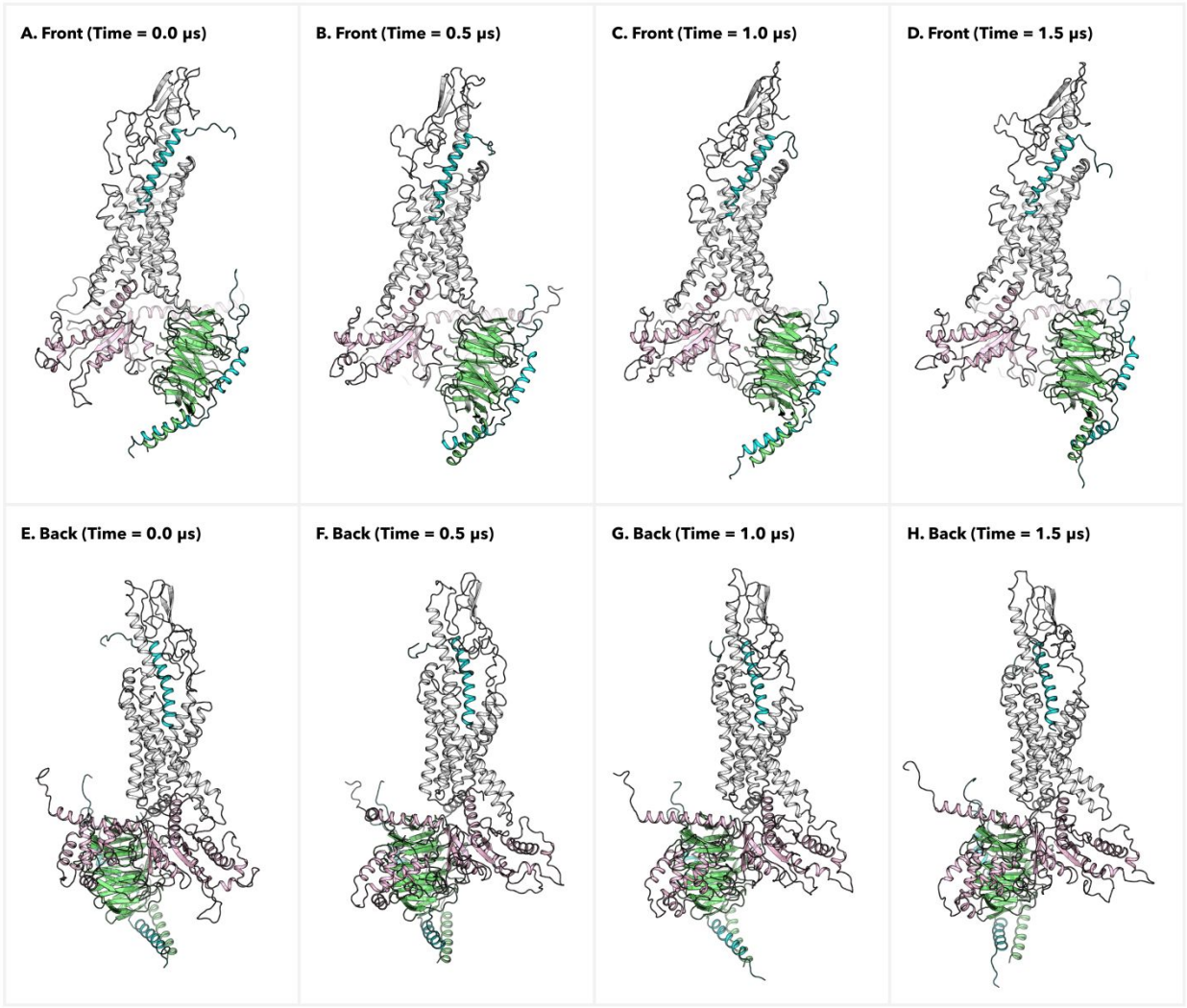

Figure S3. Structural changes of the ExP5–GLP-1R–Gs signaling complex at 0.0, 0.5, 1.0, 1.5 μs of our trajectory. (A-D) Front view. (E-H) Back view. While the overall complexation mode is stable, multiple unstructured regions, including those in GLP-1R NTD, ExP5 C-terminus and the heterotrimeric Gs protein, undergo disordered movements. The AH domain of Gαs relaxes to a slightly more downward position in the first 0.5 μs and remains stable thereafter. Other major movements are discussed in detail in the main text.

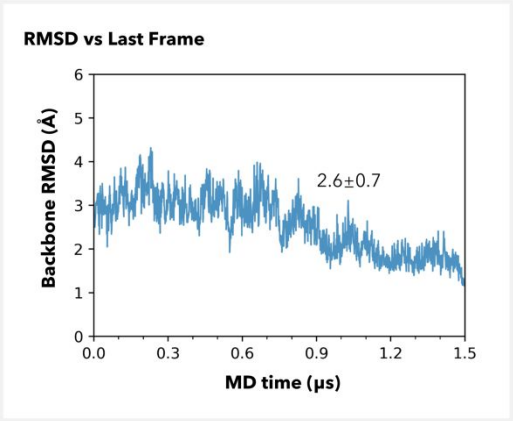

Figure S4. Backbone RMSD plot for the MD trajectory (*vs* last frame) supporting the structural integrity of the simulated ExP5-bound GLP-1R–Gs complex.

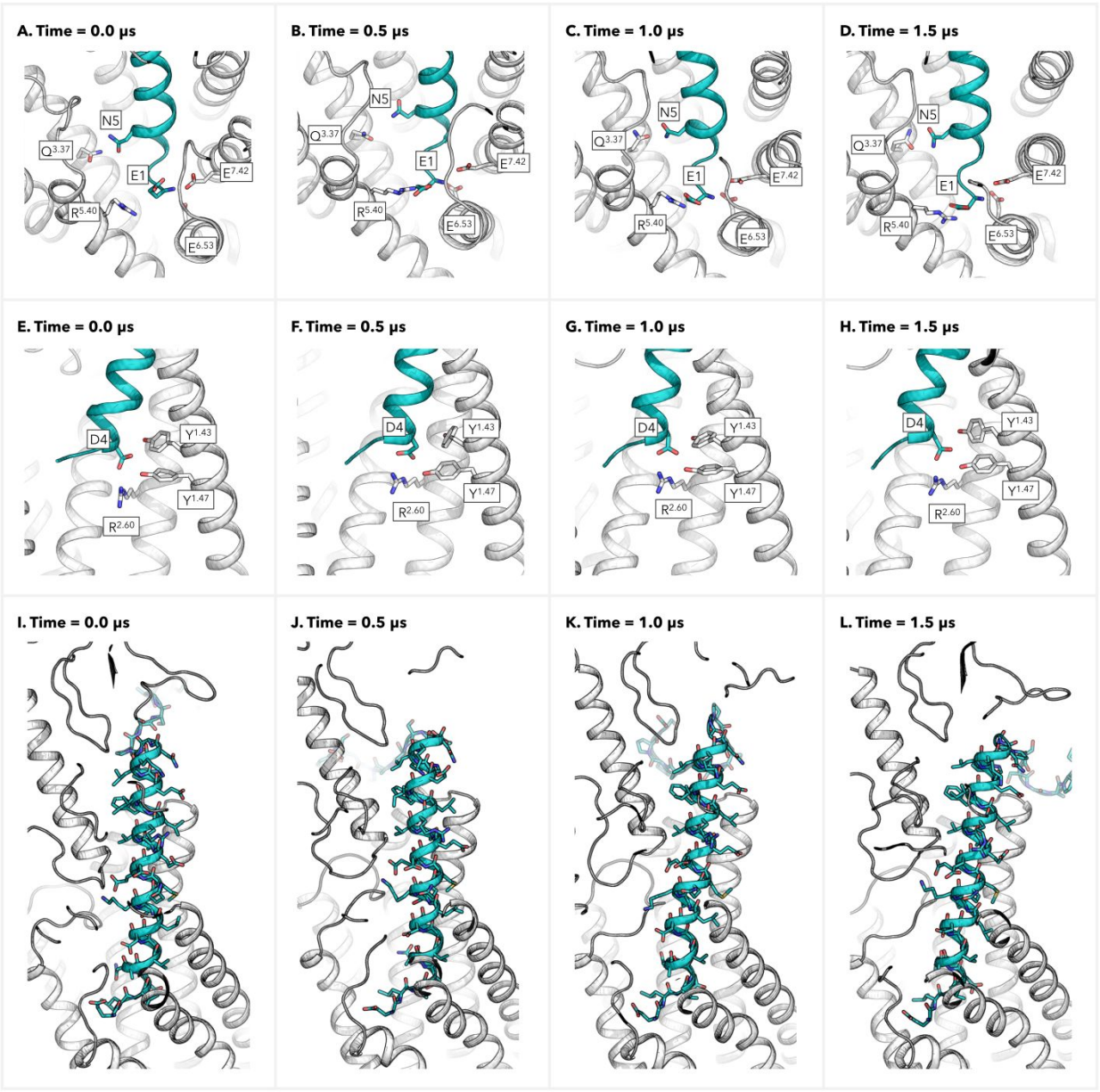

Figure S5. ExP5 binding interactions with TMD throughout our trajectory. (A-D) Front view on $E1^{ExP5}$-based SB network and $N5^{ExP5}$–$Q^{3.37}$ H-bond, suggesting that the $E1^{ExP5}$ interaction hub is established early in the trajectory and remains stable. (E-H) Side view on the $Y^{1.43}$–$D4^{ExP5}$–$R^{2.60}$–$Y^{1.47}$ HB network involving multiple synergistic anchors. (I-L) Full depiction of ExP5 atomistic motions throughout the MD simulation, which shows that the α-helical body of ExP5 maintains a stable general binding mode to GLP-1R, while the C-terminal (shown on the top) is disordered.

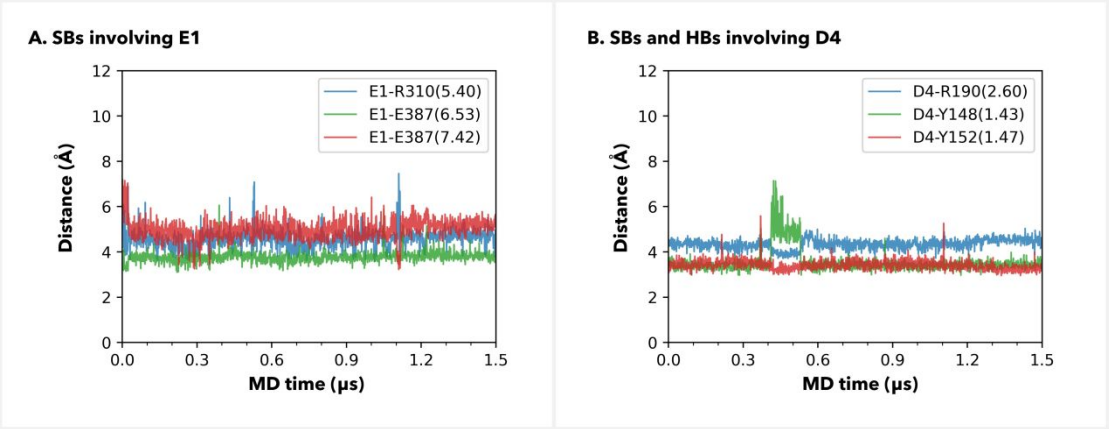

Figure S6. Simulated salt-bridge and H-bond distances for ExP5 binding interactions involving (A) $E1^{ExP5}$ and (B) $D4^{ExP5}$. See **Fig. 2** for depictions of the interactions.

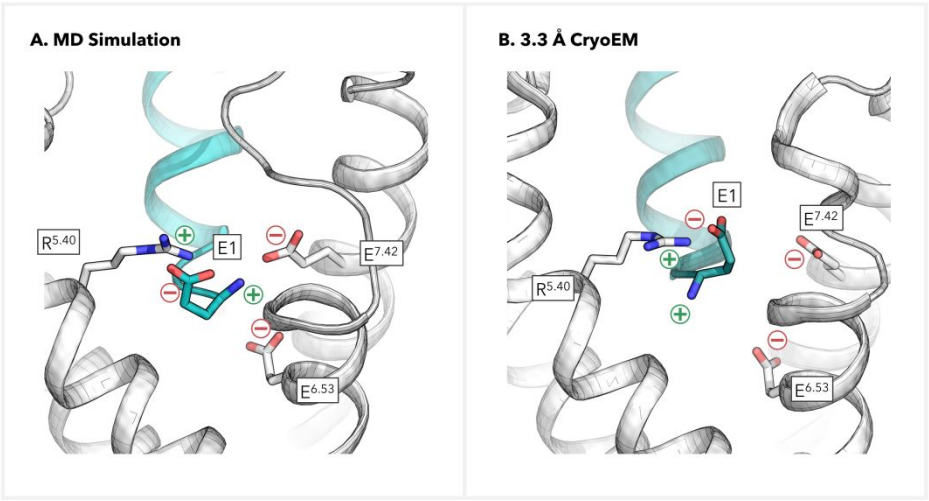

Figure S7. N-terminal $E1^{ExP5}$ interactions in (A) our current MD simulation and (B) the original cryoEM structure referenced herein (PDB code: 6B3J). The ionic engagements of $E1^{ExP5}$ by $E^{6.53}$ and $E^{7.42}$ were not captured in the cryoEM structure.

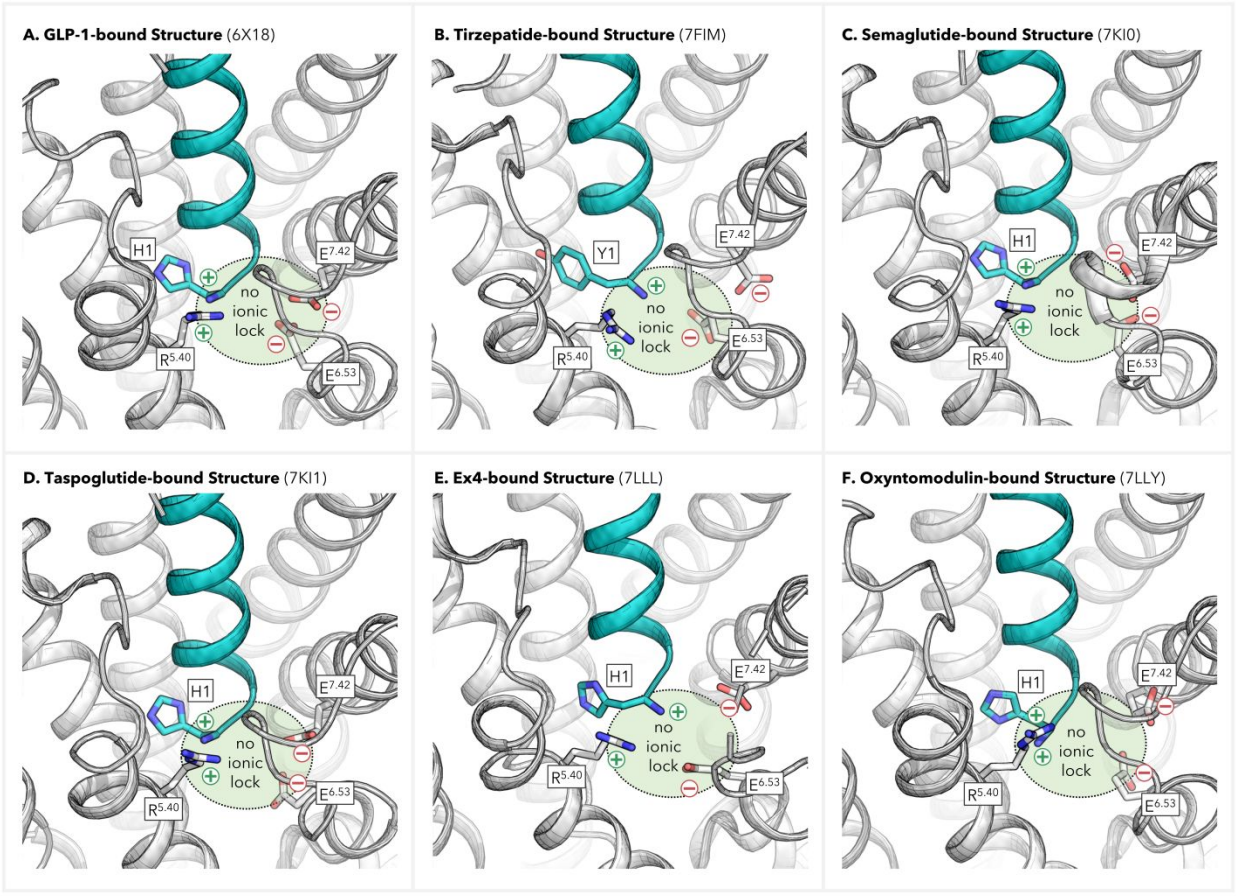

Figure S8. Binding interactions between the N-termini of peptide agonists with the GLP-1R–Gs signaling complex, showcasing the lack of the E1^{ExP5} ionic network. PDB codes are provided in parentheses.

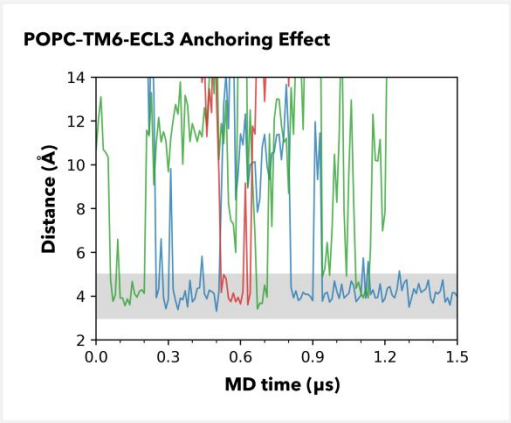

Figure S9. Simulated distances for the anchoring of POPC at the TM6–ECL3 intersection. Three POPC molecules have been observed to show significant retention time (at least 0.1 μs). For each individual POPC, we computed min[N^{POPC}–$O(A^{6.57})$, N^{POPC}–$O(F^{6.58})$] over the entire trajectory to measure the shortest distance between the positively charged N atom of POPC and the backbone O atom of either $A^{6.57}$ or $F^{6.58}$, which are presented in the current plot.

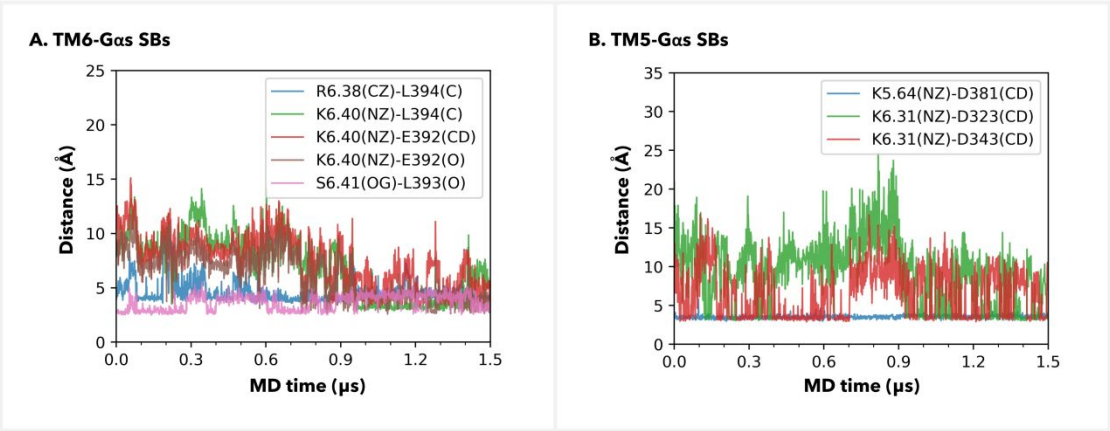

Figure S10. Simulated distances for several possible SBs at the (A) TM6-Gαs and (B) TM5-Gαs interfaces. See **Fig. 4** for depictions of these interactions.

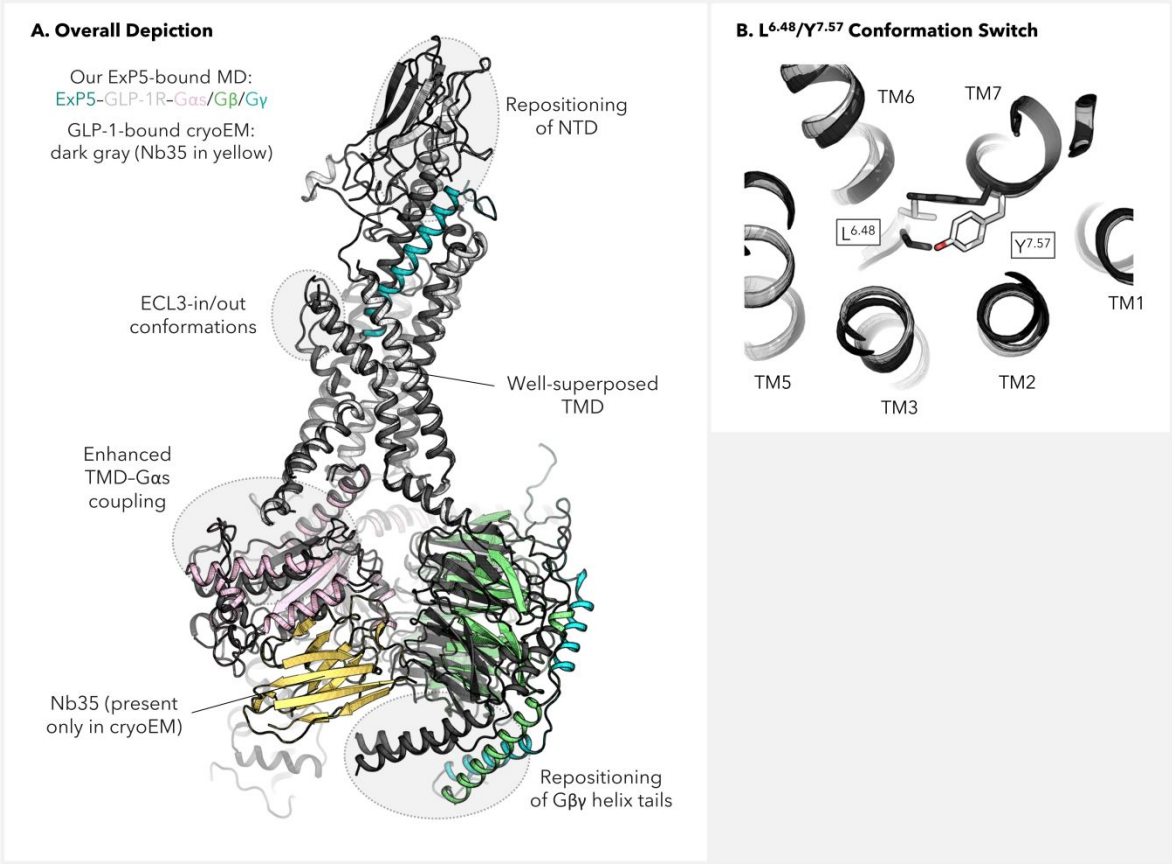

Figure S11. Superimposition of our simulated ExP5-bound GLP-1R–Gs signaling complex with a high-resolution GLP-1-bound model (PDB code: 6X18). (A) Overall depiction. (B) $L^{6.48}/Y^{7.57}$ conformation switch.